Fuel 291 (2021) 120260

Contents lists available at ScienceDirect

Fuel

journal homepage: www.elsevier.com/locate/fuel

Full Length Article

Upgraded pongamia pod via torrefaction for the production of bioenergy

Jinxia Fu [a,*], Sabrina Summers [a], Scott Q. Turn [a], William Kusch [b]

[a] Hawaii Natural Energy Institute, University of Hawaii, Honolulu, HI 96822, USA
[b] TerViva, Inc., Oakland, CA 94612, USA

ARTICLE INFO

Keywords:
Pongamia pod
Torrefaction
Fuel characteristics
Bioenergy
Physicochemical properties

ABSTRACT

Torrefaction can be used to reduce the oxygen content of biomass and improve the feedstock properties for thermochemical conversion. Pongamia (*Millettia pinnata*), a leguminous, oil-seed bearing tree, is a potential resource for sustainable aviation fuel production due to the high oil content of its seeds. The present work investigates thermochemical pretreatment of pongamia processing residues, i.e. pods. Torrefaction tests were performed with both a fixed bed reactor and a macro thermogravimetric analyzer (TGA) under nitrogen atmospheres. The effects of process conditions on feedstock properties relevant to thermochemical conversion technologies, proximate and ultimate composition, heating value, and Hardgrove grindability index (HGI), were measured. The chemical structure, reactivity, and changes in elemental composition of the torrefied materials were also investigated. The mass and energy yields decreased 43% and 25%, respectively, from the mildest (165 °C) to the most severe (281 °C) torrefaction conditions, while the energy densification index increased from 1.15 to 1.68. The HGIs of pods torrefied at temperatures >215 °C were found to equal or exceed the HGI of a reference bituminous coal sample. A LECO model TGA801 macro-TGA with a sample loading capacity of ~95 g was also used to torrefy pongamia pods. Products from the LECO and the fixed bed reactor were comparable, and the macro-TGA was demonstrated to be a useful fast screening tool to study effects of process parameters.

1. Introduction

With the cost reduction in renewable energy technologies and advances in digital technologies, the contributions of renewables to meet global final energy consumption are projected to increase from ~42 TJ in 2019 to ~95 TJ in 2040 [1]. The renewables share of global heat demand is expected to reach 39 TJ in 2040 and biofuels are projected to account for ~9.4 TJ to the transportation sector [1]. Sustainable carbon from biomass is an important source for energy and chemical production and is recognized as a future solution for reducing anthropogenic greenhouse gas (GHG) emissions. The use of agricultural residues for energy purposes, in particular, has become a new research focus in the past few decades [2,3]. The use of biomass as an energy feedstock has several recognized disadvantages, e.g. heterogeneity, high moisture and oxygen content, low energy density, poor biological stability, presence of contaminants etc. [2–4]. Thus, pre-treatment offers possible solutions to overcome these technical issues.

Torrefaction is a thermochemical treatment method conducted at 200–300 °C, at atmospheric pressure, and in the absence of oxygen [5]. The main objective is to reduce the oxygen content of the torrefied product compared to the parent biomass [4–7]. In general, torrefaction of woody biomass materials results in mass and energy yields of 70% and 90%, respectively. Consequently, energy densification (mass basis) improvement by a factor of 1.3 are typical [5]. The mass fraction of the parent biomass volatilized during torrefaction (~30%) has a low energy content, i.e. ~10% of the total energy [4]. Torrefied materials generally possess higher energy density, better grindability, better hydrophobicity and biological stability, which can reduce transportation costs, feedstock preparation and storage costs and thus the overall cost of the final product [4–6]. In addition, the torrefied biomass should have lower hydrogen/carbon (H/C) and oxygen/carbon (O/C) ratio compared to the raw biomass.

Improvement is needed to achieve commercialization of biomass torrefaction technologies. Lab-scale investigations performed in the past few decades focused on the impacts of operating conditions on the feedstock properties of the torrefied products [4,6,8]. Lab-scale torrefaction is usually conducted utilizing micro-thermogravimetric analyzers (TGA) [8–11] or small bench scale reactors [12–17]. The advantages of the micro-TGA method include: (1) easy to conduct; (2) capable of monitoring the mass change during the entire torrefaction

* Corresponding author.
E-mail address: jinxiafu@hawaii.edu (J. Fu).

https://doi.org/10.1016/j.fuel.2021.120260
Received 3 December 2020; Received in revised form 13 January 2021; Accepted 15 January 2021
Available online 6 February 2021

process; and (3) possible identification of volatile organic compounds when combined with a mass spectrometer (MS). The limitation of a TGA in comparison with a bench-scale reactor, however, is that insufficient torrefied material is produced for subsequent characterization, e.g. grindability, heating value, element content, etc. Thus, future studies are needed to develop systems capable of generating sufficient materials for characterization as well as monitoring mass change.

Millettia pinnata, also known as pongamia or karanja, bears seed pods that partition in a ratio of 40:60, seed:pod by mass (dry). Pongamia has applications for biomedicine and energy production [18]. The pongamia tree has been traditionally used to treat diseases and wounds [19–21], its leaf extract has antipyretic and muscle relaxant effects [22], and its leaves also exhibit corrosion inhibition properties [23]. The pongamia seed oil has been used for biofuel production and as biopesticide for crop protection [24–26]. Although the pongamia seed cake remaining after oil extraction has a nitrogen content of 0.9–7.2 %wt [27], its application for animal feed is limited due to the presence of anti-nutritional species, e.g. karanjin (CAS# 521-88-0), pongamol (CAS# 484-33-3), and glabrin (CAS# 35024-30-7) [28,29]. Thus, pongamia seed cake has been mainly used as solid fuel [30,31] and fertilizer [32]. Torrefaction pretreatment of the cake has also been investigated [31,33,34]. Studies on pongamia pod, which is typically disposed after seed separation, however, are limited. Ujjinappa and Sreepathi employed the pongamia pod for production of blended fuel briquettes and found them to have higher fixed carbon content and calorific value in comparison with agricultural residue briquettes [35]. The pongamia pods were also utilized to produce activated carbon, which was demonstrated to have high surface area, 156.83 m^2/g [36]. Torrefaction studies on pongamia pod as a coproduct, however, have not been reported in the literature.

The present work investigates the impact of torrefaction pretreatment on the fuel characteristics of pods collected from pongamia trees grown on the island of Oahu, Hawaii, USA. Torrefaction tests were initially performed with a conventional fixed bed reactor shown in Fig. 1 under nitrogen atmospheres. The essential properties of fuel used in thermochemical conversion, including proximate and ultimate composition, heating value, and Hardgrove grindability index (HGI) [37], were measured to evaluate the influences of torrefaction conditions. The chemical structure, thermal decomposition process, and elemental composition of the torrefied materials were also investigated using Fourier-transform infrared spectroscopy (FTIR), micro-TGA, and X-ray fluorescence (XRF), respectively. Moreover, a state-of the art macro-TGA method, which can monitor the mass loss process as well as produce sufficient materials for characterization afterwards, was also developed as a rapid screening tool to study effects of torrefaction process parameters. The performance of a macro-TGA was also compared with that of the conventional fixed bed reactor.

2. Materials and methods

2.1. Materials

Pongamia seed pods were provided by TerViva Inc. and collected in May 2016 from Hawaii Agriculture Research Center, Kunia, HI (21°22′58.9″N, 158°02′21.8″W) (TerViva Planting). The seed pods were hand harvested from trees and then 1) soaked in a chlorine/water solution (bleach water) for 1 min, 2) placed on a mesh screen and dried in full sun for 2–3 h, and 3) stored in an air conditioned room at ~21 °C in loosely woven mesh bags. The bleach water treatment is used by TerViva to preserve seed quality and prevent mold formation during storage, but is unlikely to be used in commercial practice. The pods (Fig. 1) were hand separated from the seeds and milled to <2 mm particle size using a FRITSCH Universal Cutting Mill "Pulverisette 19" (Idar-Oberstein, Germany). A bituminous coal was obtained from a Hawaii power plant on the island of Oahu, Hawaii, USA.

2.2. Torrefaction methods

Torrefaction tests were performed using a fixed bed reactor and a macro-TGA.

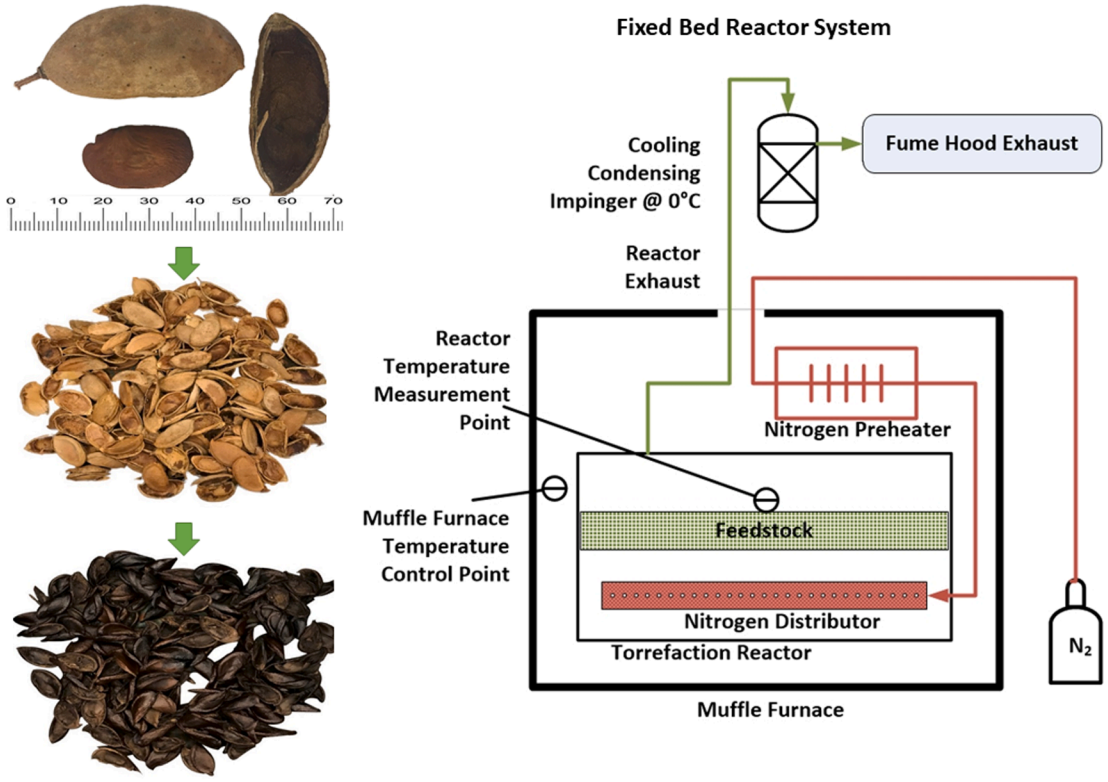

Fig. 1. Pongamia seed, pod, and torrefied pod, and schematic of the fixed bed reactor: the unit of the scale is mm.

2.2.1. Fixed bed reactor method

A schematic of the square fixed bed reactor test bed [38] is shown in Fig. 1. The reactor had dimensions of 25x25x7 cm and was constructed from mild steel. Approximately 100 g of pongamia pods (<2 mm) were evenly distributed over a 140-mesh stainless steel screen supported 25 mm above the reactor floor. The reactor was sealed and placed in a Fisher Scientific Isotemp 650–58 muffle furnace (New Hampshire, USA). To maintain an inert atmosphere within the reactor, nitrogen gas (N_2) at a rate of 1.2 L/min was supplied to the bottom of the reactor and released through a perforated coil (~1.1 m long, 6 mm (OD) copper tube). The N_2 was preheated by passing through a ~1 m long, 6 mm (OD) copper tube placed inside of the muffle furnace. The muffle furnace was programmed for a heating rate of 20 °C/min to the target torrefaction temperature. The outlet of the reactor was connected to a stainless steel impinger containing 500 mL of 2-propanol placed in a container of ice water to remove condensable species from the exiting gas stream. The reactor was maintained at the target torrefaction conditions for 60 min and then cooled in the open furnace for ~1 h while maintaining the N_2 flow.

2.2.2. Macro-TGA method

A macro TGA (TGA801, LECO Corporation, St. Joseph, MI) was also used to perform torrefaction tests. This system is designed to conduct proximate analysis of 19, ~1 g biomass samples in ceramic crucibles. An empty crucible (number 20) serves as a reference. The crucibles are held in a circular carousel and the mass change of each sample is monitored throughout the analysis by automatically rotating its crucible to a position above a balance pedestal. Each measurement takes 12–15 s. The recording frequency of each sample mass, therefore, depends on the number of crucibles loaded, e.g. approximately 4 min are needed when the sample carousel is fully loaded with 20 crucibles, i.e. 19 with samples and one reference. The ~19 g of parent biomass across all of the crucibles does not yield sufficient torrefied material for complete property analysis. Ideally, the sample loading capacity of the macro-TGA would equal that of the fixed bed reactor, i.e. ~100 g. To explore this, sample mass was increased from 1 g to 5 g to evaluate the macro-TGA system as a rapid screening tool for torrefaction process conditions. Note that 5 g per crucible approaches the maximum loading capacity of pongamia pods owing to the size limitation of the crucibles. Preliminary tests were conducted with 1, 2, 3, 4, and 5 g sample loading to ensure that process results were independent of initial sample mass.

For the pongamia pod torrefaction tests, approximately 95 g of pongamia pods (<2 mm) were loaded into 19 ceramic crucible (~5 g each) and covered with the matching lid (Part #621–331 and 529–048, respectively, LECO Corporation). Macro TGA tests were performed with the same heating program as the fixed bed reactor, i.e. (1) heating rate of 20 °C/min, (2) 60 min residence time, and (3) 60 min cooling period. The N_2 flow rate was set at 10 L/min during heating, holding, and cooling process. Note that the N_2 sweeps volatile products from the common head space above the crucibles. As the impact of N_2 flow rate on the torrefaction solid products is negligible [39,40], given the larger sample mass and larger volatile matter release, the maximum allowed flow rate, i.e. 10 L/min, was selected for performing the macro-TGA torrefaction tests in order to protect the electronics inside the reaction furnace and ensure accuracy of the weighing process.

2.3. Property determination

2.3.1. Hardgrove grindability index (HGI)

The grindability of the raw and torrefied pongamia pods was determined using a modified volumetric HGI method [16] based on ASTM D409/D409M-16 [37]. A 50 cm^3 sample was placed into a 500 mL stainless steel milling cup with 25, 20 mm stainless steel balls and milled for 2 min at 165 rpm (Retsch PM100, Düsseldorf, Germany). The HGI is based on the fraction of sample that passes a 75 μm sieve after 5 min of shaking (W.S. Tyler Ro-Tap RX-29, Ohio, USA).

$$\mathrm{HGI} = a + bx \quad (1)$$

where $\times$ is the mass percentage of sample passing the 75 μm sieve, and a and b are constants determined from standard reference coal samples with known HGI value [16]. Four reference coal samples with HGI of 27, 47, 64 and 89, were purchased from the Australian Coal Preparation Society's (ACPS) CHOICE Analytical Pty Ltd, and the constant a and b determined is 16.6 and 1.43, respectively, with an r^2 value of 0.996. After the nondestructive grindability tests, samples were milled to < 0.2 mm using an ultra-centrifugal mill (Retsch ZM200, Düsseldorf, Germany) for the tests listed below.

2.3.2. Proximate analysis

The proximate analysis was performed using a macro thermogravimetric analyzer (TGA801, LECO Corporation, St. Joseph, MI) based on ASTM E1756, E872 and E1755 for moisture, volatile matter, and ash content determination, respectively [41–43].

2.3.3. Ultimate analysis

A LECO CHN628 (LECO Corp., St. Joseph, MI) was employed to determine the carbon, hydrogen, and nitrogen content of the torrefied materials. Approximately 90 mg samples were analyzed using furnace and afterburner temperatures of 950 and 850 °C, respectively.

2.3.4. XRF analysis

Quantitative elemental analysis of the parent pods and the torrefied materials was performed using a Bruker S8 TIGER XRF spectrometer (Bruker Corp., Billerica, MA) to determine the ash-forming elements. The details on pellets preparation and XRF system parameters were described in a previous publication [18]. Spectrum recording and evaluation were performed with the Quant-Express software using the best detection mode (Bruker AXS).

2.3.5. Micro-TGA analysis

Reactive characteristics of the raw and torrefied pods were investigated with a micro-thermogravimetric analyzer (micro-TGA) (TA Instruments SDT Q600, Delaware, USA). The micro-TGA experiments were performed under atmospheric pressure with the flow of 100 mL/min argon. A 6–10 mg sample was evenly loaded into an alumina sample cup (TA Instruments, 960070.901). The micro-TGA system was programed with (1) start temperature of 50 °C and heating rate of 10 °C/min; (2) a 30 min isothermal hold at 110 °C to remove moisture from the sample; and (3) a heating rate of 10 °C/min to a final temperature of 800 °C.

2.3.6. Fourier transform infrared spectroscopy (FTIR)

Infrared spectra were generated and recorded using a FTIR equipped with attenuated total reflectance (ATR) sampling accessory (Thermo Scientific Nicolet iS 10, Massachusetts, USA). Approximately 1–2 mg of milled sample (<0.2 mm particle size) was pressed against a diamond crystal using a spring-loaded press and all the spectra were obtained over the wavenumber range from 4000 to 650 cm^{-1} with 64 scans at 2 cm^{-1} resolution.

2.3.7. Higher heating value

A Parr 6200 Isoperibol Calorimeter (Parr Instrument Company, Moline, IL) was used to measure the heat of combustion based on ASTM D4809-18 [44] and reported as the high heating value (HHV).

2.3.8. Composition analysis

The chemical composition of pongamia pod, i.e. cellulose, hemicellulose, and lignin content, was determined according to the National Renewable Energy Laboratory (NREL) procedure [45].

2.4. Data processing

Performance indicators for the torrefaction process were calculated according to the following equations,

$$M_y(\%) = \frac{m_{tor}}{m_{raw}} \times 100 \quad (2)$$

$$I_{ed} = \frac{HHV_{tor}}{HHV_{raw}} \quad (3)$$

$$E_y(\%) = M_y \times I_{ed} \quad (4)$$

where M_Y and E_Y are mass and energy yields, respectively; I_{ed} is the energy densification index; m is the mass of the material, and HHV is the higher heating value. Subscripts *raw* and *tor* are raw and torrefied biomass, respectively.

The release ratio of elements via torrefaction was calculated based on XRF analysis results according to equation (5),

$$\text{Release Ratio}(\%) = \frac{C_{raw} - C_{tor} \times \frac{M_y}{100}}{C_{raw}} \times 100 \quad (5)$$

where C is the concentration of element determined by XRF analysis.

3. Results and discussion

3.1. Fixed bed reactor

The pongamia pods are light brown, 3–6 cm long and 1–2 cm wide (Fig. 1). Their (cellulose + hemicellulose) and lignin contents are 51.73 and 21.71 %wt, respectively. Torrefaction tests of pongamia pod were performed in a fixed bed reactor at 165, 184, 210, 215, 230, 254, and 281 °C with the corresponding furnace temperatures of 180, 200, 225, 235, 250, 275, and 300 °C, respectively. The color of the torrefied pod gradually turns from light brown to black with the increase of torrefaction temperature (shown in Fig. 2, particle size = 0.2 mm). Fig. 3 illustrates the impacts of torrefaction temperature on the process yields and the energy densification index (I_{ed}). The mass and energy yields decrease linearly as torrefaction temperature increases from 184 to 281 °C. The I_{ed}, reflecting the energy content change, increases linearly over the same temperature range. The torrefaction results at 165 °C were not included in the linear regression calculation (Fig. 3), as the temperature was too low to significantly impact the material properties. Using the regression equation, the mass yield reached a 70% target value [5] when the torrefaction temperature is approximately 225 °C. Corresponding energy yield (90.75%) and I_{ed} (1.32) values are also close to targeted values, 90% and 1.30, respectively [5]. Based on the process yield and energy content change, the preferred torrefaction temperature for 2 mm pongamia pod material is 220–230 °C at a residence time of 60 min.

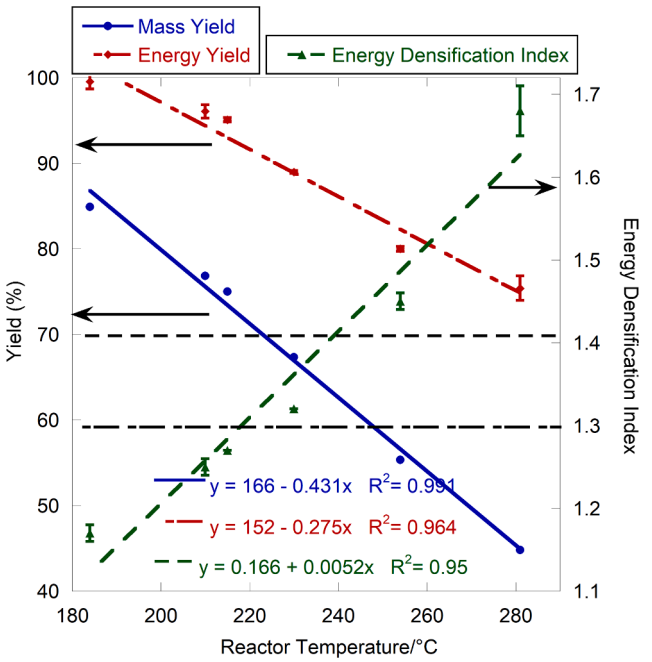

Fig. 3. Torrefaction performance of the fixed bed reactor in a temperature range of 184–281 °C.

Torrefaction performed on whole pods at 208 °C (furnace temperature 225 °C) produced similar mass and energy yields and I_{ed}, (76.02%, 95.86%, and 1.26, respectively) were obtained as the tests conducted at 210 °C (furnace temperature 225 °C) with < 2 mm size pod, 76.86%, 96.06%, and 1.25, respectively. Torrefaction of whole pods would be comparable to wood chip particle sizes cited in the literature for

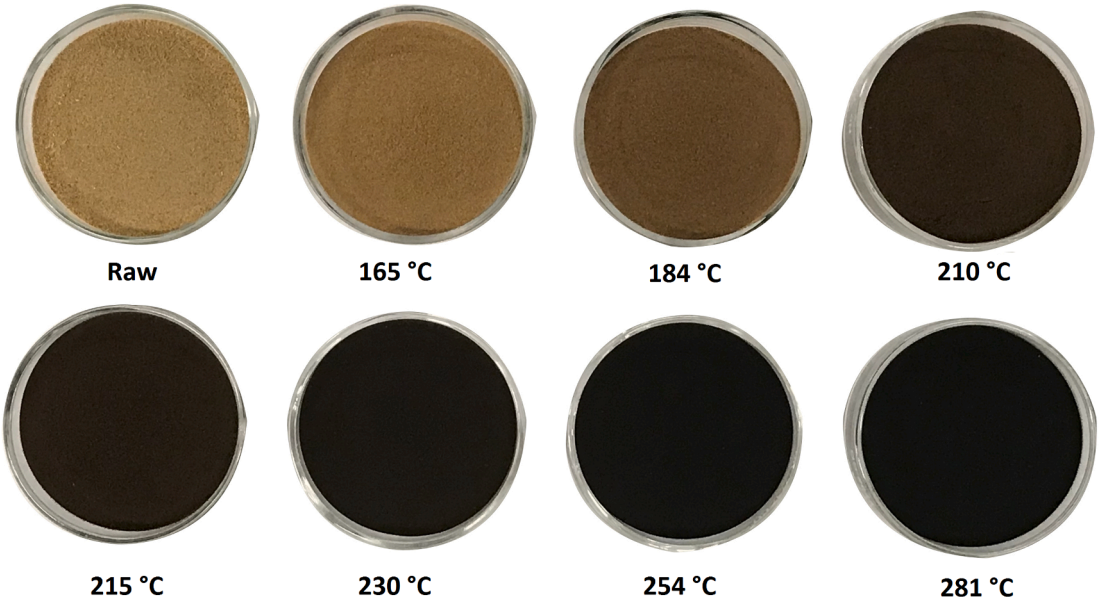

Fig. 2. Torrefied pod obtained from the fixed bed reactor tests.

industrial applications.

The influences of torrefaction temperature on physicochemical properties and structure of the pongamia pods were also investigated. Fig. 4 compares the proximate analysis results of the pods, torrefied pods and a bituminous coal sample from a power plant in Hawaii; data and error estimates are presented in Table S1 of the supplementary materials. As expected, the fixed carbon (FC) and ash contents of the torrefied materials increases linearly over the torrefaction temperature range ($FC\ \%wt = -26.2 + 0.249 \times T/°C$, $R^2 = 0.969$ and $Ash\ \%wt = -5.54 + 0.0642 \times T/°C$, $R^2 = 0.948$), whereas the volatile matter (VM) content exhibited an opposite trend, $VM\ \%wt = 132–0.313 \times T/°C$, $R^2 = 0.970$. As with Fig. 3, these regression equations omit the data for the 165 °C torrefaction temperature. The increase of fixed carbon and ash fraction is attributed to the loss of volatile matter during the torrefaction process. The mass yield and proximate analysis data at any of the torrefaction temperatures verify that volatile matter loss, not secondary fixed carbon formation, accounts for the increased fixed carbon concentration. The fixed carbon content of the torrefied pods increased to 44.75 %wt at a process temperature of 281 °C, close to the fixed carbon content of the bituminous coal sample, 45.75 %wt. The volatile matter content of the torrefied pod, 42.88 %wt, is ~3.5% (absolute) lower than that of the bituminous coal.

Ultimate analysis results of torrefied pods are shown in Fig. 5 (A) and (B); complete data and error estimates are presented in Table S1. The oxygen content was calculated by subtracting the carbon, hydrogen, nitrogen, sulfur, and ash content from 100. In comparison to the parent material, the torrefied biomass possesses increased carbon and decreased oxygen and hydrogen content due to the release of volatile matter rich in hydrogen and oxygen. When the torrefaction temperature is 281 °C, the carbon content of the torrefied pod, 63.42%, is ~8% (absolute) lower than that of the bituminous coal, 72.20 %wt, and the oxygen content, 17.68 %wt, is only ~5% higher than the value of bituminous coal, 12.49 %wt (Fig. 5 (A)). Carbon content linearly increased with torrefaction temperature, whereas the oxygen content declined (Fig. 5 (A)). Nitrogen is nonvolatile at the mild torrefaction temperatures and is enriched in the torrefied products. Fig. 5 (B) shows the torrefied pod data overlaid onto a Van Krevelen diagram. The element ratios gradually shifted away from biomass towards coal with the increase of torrefaction temperature. The torrefied pod has similar chemical composition, i.e. H/C and O/C, as peat when the torrefaction temperature increased to 210 °C, and the pods can be further torrefied to a fuel like lignite when the torrefaction temperature is at 254 °C. The torrefied pod is expected to have similar fuel qualities as coal when the torrefaction temperature is 281 °C.

Fig. 6 displays the impacts of torrefaction temperature on the energy content and grindability of the torrefied pods. A torrefaction temperature of 281 °C yields a product with HHV of 27.26 MJ/kg, close to the value of the bituminous coal sample, 28.18 MJ/kg. The grindability of the torrefied pods was improved owing to the embrittlement of the material and breakdown of hemicellulose during the torrefaction process [7]. The HGI of the torrefied pods was also found to increase with the torrefaction temperature, but polynomially over the temperature range (184–281 °C), achieving a HGI comparable to bituminous coal at a treatment temperature of ~220 °C. The HGI of the raw pods with particle size < 2 mm, 27.53, increased almost five-fold when torrefied at 281 °C.

XRF analysis was performed to determine the elemental composition of the raw and torrefied pods; data and error estimates for all elements detected are presented in Table S2. The limit of detection (LOD), defined as the minimum detectable concentration of an element in the wax pellet/matrix, calculated here as the average LOD from all measurements on the torrefied pods from the fixed bed reactor and LECO macro-TGA. Samples with element concentrations higher than the LOD are reported. Table S3 includes the XRF-based total oxides (ash content) calculated by two different matrices, i.e. $C_6H_{10}O_5$ [18,46,47] and the matrix derived from the ultimate analysis results. The ash content of the torrefied pods based on XRF analysis and the $C_6H_{10}O_5$ matrix is closer to that obtained by proximate analysis (RMSE = 0.58 %wt) than the ash content based on the same XRF data and the ultimate analysis matrix (RMSE = 1.40 %wt). The element concentrations listed in Table S2, therefore, were calculated using $C_6H_{10}O_5$ matrix.

Although the fuel properties of the pods are markedly improved by torrefaction, the thermochemical conversion of torrefied pods remains challenging owing to high concentrations of alkali metals. Fig. 7 (A) presents the major element content (>1,000 ppm by mass) of the torrefied pods quantified by XRF. These major elements are in nonvolatile

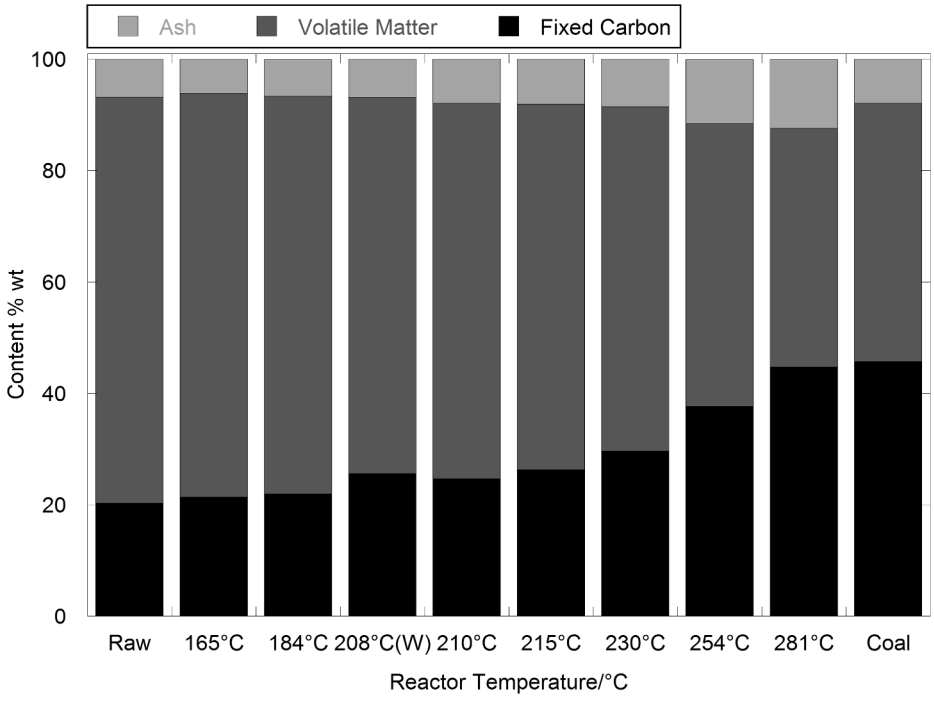

Fig. 4. Proximate analysis results of the torrefied pods.

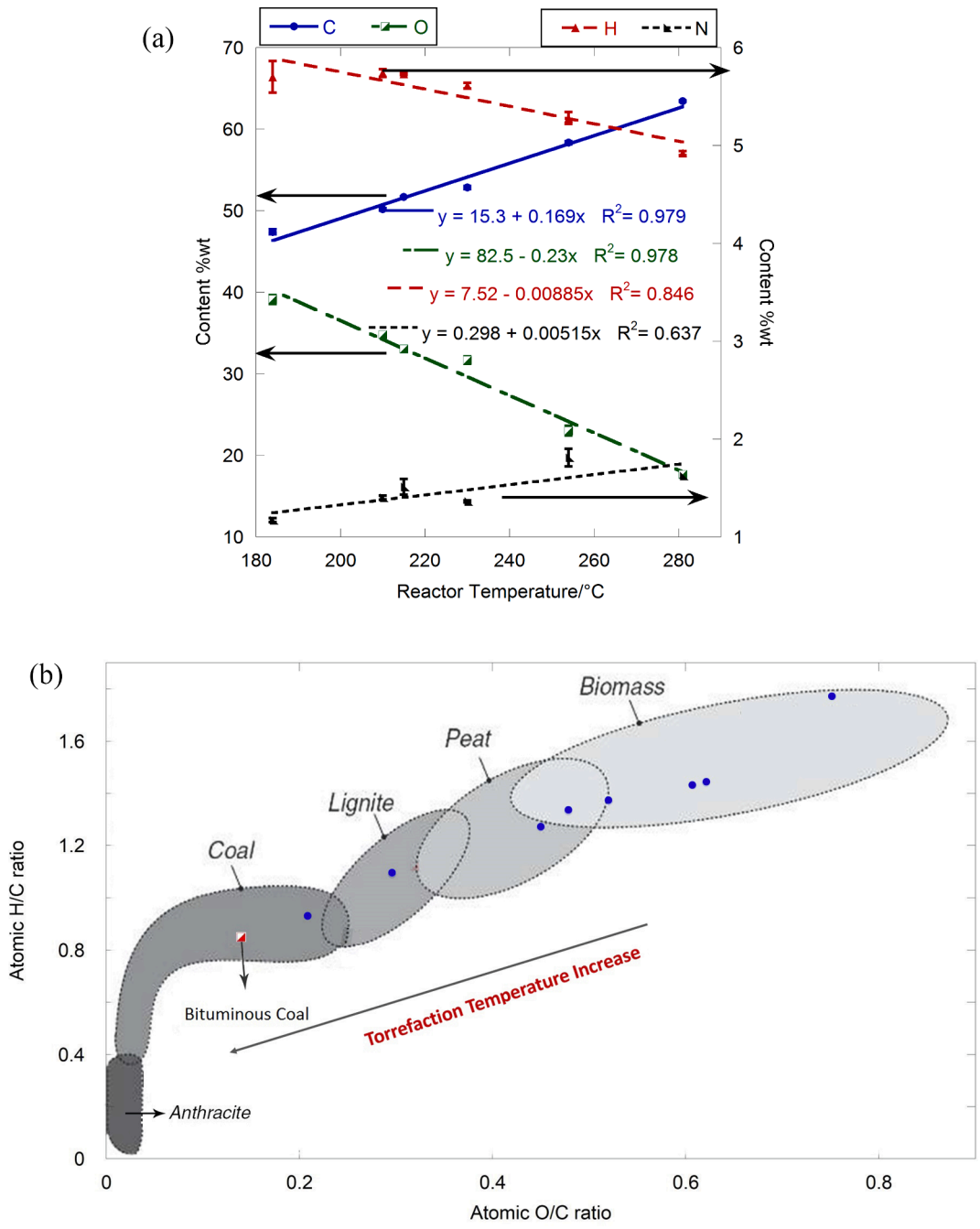

Fig. 5. Ultimate analysis results of torrefied pods: (A) relationships between the C, H, N, O contents with torrefaction temperature; (B) Van Krevelen diagram.

form in the torrefied pods and increase with torrefaction temperature. The concentration of alkali and alkaline earth metals, i.e. sodium (Na), magnesium (Mg), potassium (K) and calcium (Ca), in the torrefied pods were found to change linearly with the torrefaction temperature in the range of 184–281 °C. It has been reported that Cl and K content of biomass can be reduced via torrefaction and that the release ratio of Cl and K increases with torrefaction temperature [48,49]. This was not observed in the present study, as Cl and K concentrations linearly increased with torrefaction temperature. Differences with the literature reports are likely due to their smaller particle sizes (<0.5 mm), higher torrefaction temperatures (350 °C), and a non-static fuel bed, all contributing to improved mass transfer. Different from Cl and alkali metals, sulfur (S) was released from the pods during torrefaction, although the total S concentration increased with torrefaction temperature. Fig. 7 (B) shows the relationships between the release ratio of S calculated based on equation (5) and torrefaction temperature. The release ratio of S generally increases with torrefaction temperature, and approaching ~30% at 281 °C. In addition, the S release ratio of the pod at 254 °C, ~27%, agrees with that reported for miscanthus and spruce bark torrefied at 250 °C, 24 and 23.1%, respectively [49]. S contents of the three biomass materials reported by Saleh et al. ranged from 270 to 1301 ppm indicating that its release ratio during torrefaction appears independent of initial concentration [49]. Note that S released under torrefaction conditions is thought to be associated with the organic sulfur [45], and would form H_2S [50], which can be removed from the off gas stream using readily available commercial processes such as iron sponge sorption, activated carbon beds, or amine solutions [51].

Thermogravimetric (TG) and derivative thermogravimetric (DTG) analyses of the raw and torrefied pods were conducted by micro-TGA, and the results are shown in Fig. 8. In general, mass loss has three

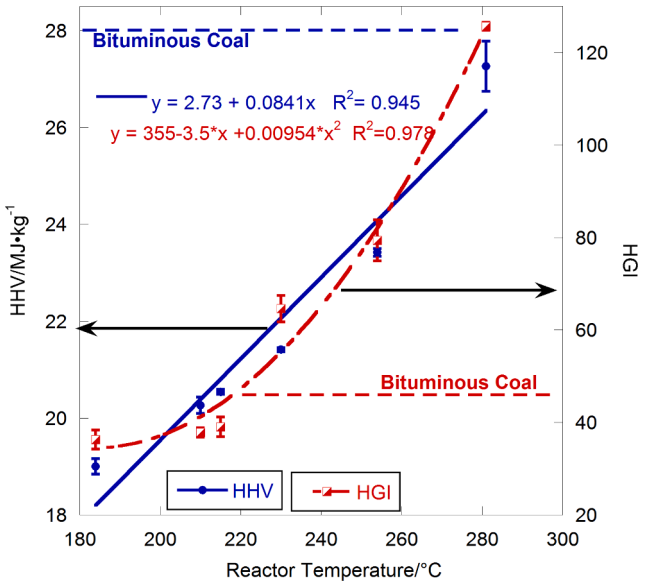

Fig. 6. Higher heating value and Hardgrove grindability index of the torrefied pods.

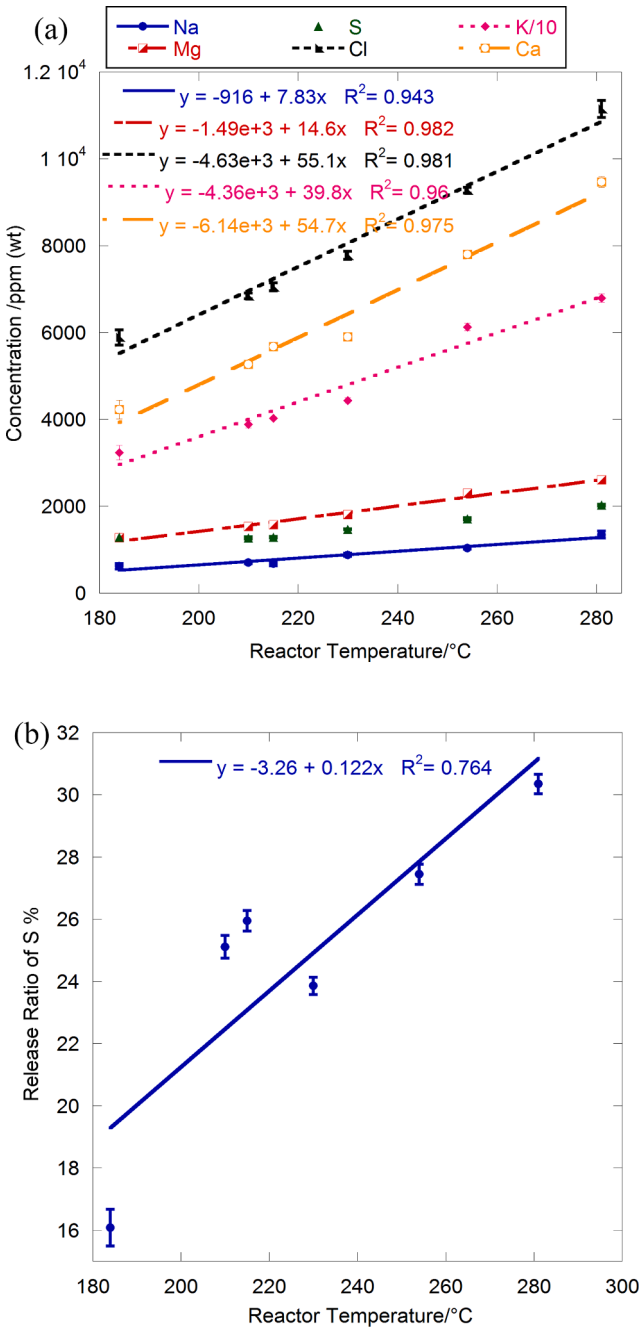

Fig. 7. XRF elemental analysis results of torrefied pods: (A) concentration of major elements; (B) release ratio of sulfur.

stages: (1) 1st stage (T < 200 °C) with slightly reduced mass, usually < 10 %wt; (2) 2nd stage (200 < T < 500 °C) with significant drop in mass; (3) 3rd stage (T > 500 °C) with limited weight loss [9]. The mass loss is mainly attributed to (1) drying and releasing of some light volatile species at the 1st stage; (2) decomposition of hemicellulose, cellulose and lignin at the 2nd stage; (3) degradation of other heavy components (mainly unreacted lignin [52]) at the 3rd stage [9]. As with the results obtained from proximate and ultimate analysis, torrefaction at 165 °C did not have significant impact on the pod reactivity. For the raw pods, the mass loss at the 1st stage is < 5 %wt, whereas mass loss at the 2nd stage is approximately 60 %wt (Fig. 8 (A)). The major decomposition of hemicellulose and cellulose occurs at 180–360 °C (Fig. 8 (B)). The 1st stage mass loss of the torrefied pods is similar to that of the raw materials, whereas the weight loss fraction of the torrefied pods at the 2nd stage span a range of 30–60 %wt (absolute) and decreases with the torrefaction temperature. The onset temperature of the 2nd stage decomposition for torrefied pods, however, increases with torrefaction temperature and shifts from 186 °C for raw materials to ~300 °C for pods torrefied at 281 °C. This shift results from the removal of volatile species/gases during the torrefaction process. Correspondingly, the temperature of maximum mass loss rate shifts from 308 °C to 393 °C as torrefaction temperature increases from 165 °C to 281 °C. In addition, the amounts of residue at the end of the 3rd stage (500 °C) increased with torrefaction temperature, from 35 %wt to 65 %wt of initial sample mass at 165 °C and 281 °C, respectively. Note that part of the hemicellulose and cellulose was also removed by torrefaction at a temperature > 254 °C, as reflected by the significant reduction of peak height, i.e. mass loss rate for the torrefied pods. As expected, the TG and DTG curves approach that of bituminous coal at higher torrefaction temperatures.

The chemical structure of the raw and torrefied pods was investigated using FT-IR. Fig. 9 shows the absorption spectroscopy of raw and torrefied pods. For the torrefied pods, the intensity of the OH bands at 3307 cm^{-1} decreases with increasing torrefaction temperature owing to the decomposition of carbohydrates, and the peak almost disappears for torrefaction temperatures ≥ 254 °C [14,53]. Conversely, the CH_2– and C = C stretching peaks (2918 and 1604 cm^{-1}, respectively) significantly increase with torrefaction temperature, illustrating these fractions are not significantly affected by the torrefaction process and may become more concentrated owing to the removal of other fractions, i.e. hemicellulose [8,53]. As expected, the intensity of C-O stretching band at 1031 cm^{-1}, associated with carbonyl groups of hemicellulose or dehydrated cellulose, decreases with increased torrefaction temperature, and may result from the removal of acetyl groups [53]. This is consistent with the ultimate analysis results, i.e. the oxygen content of the torrefied materials decreases with the increase of torrefaction temperature.

The preliminary torrefaction tests were performed with a fixed bed reactor in a temperature range of 165–281 °C with 60 min hold time and cooling period, and the results indicate that the torrefaction process can pronouncedly improve the fuel qualities of pongamia pods, and the particle size reduction of the raw pods isn't necessary. The mass and energy yields and energy densification index can reach targeted values, 70%, 90%, and 1.30, respectively, at torrefaction temperatures of 220–230 °C. The torrefied pods possess similar fuel qualities as bituminous coal at a torrefaction temperature of 281 °C, at which the oxygen

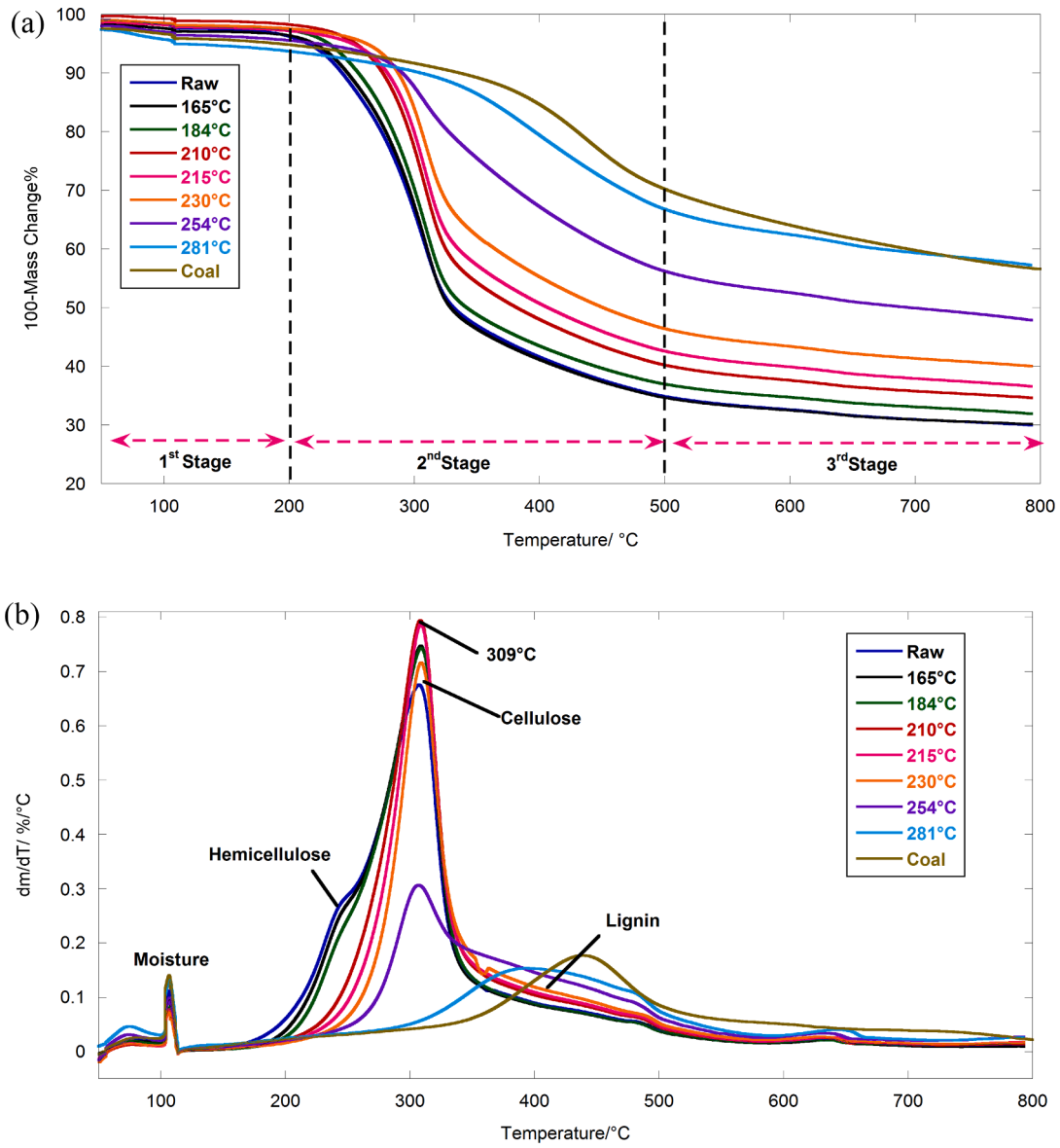

Fig. 8. Micro-TGA analysis of torrefied pods: (A) thermogravimetric curve; (B) derivative thermogravimetric curve.

content will be less than 20 %wt. The mass loss in the torrefaction process is mainly attributed to the chemical decomposition of hemicellulose, which is demonstrated by the TG and chemical structure analysis performed by micro-TGA and FT-IR, respectively. In addition, sulfur was found to slowly release from the pod during the torrefaction process, but the torrefied materials still have increased sulfur content in comparison with the raw pods. The release of chlorine during torrefaction, however, was not observed. The further elevated concentration of alkali metals and Cl will require attention if the torrefied pods are considered for combustion and gasification applications [54,55], and other pretreatment of the pods, e.g. water leaching, may be needed.

3.2. Macro-TGA

The LECO TGA 801, was also employed for torrefying the pongamia pod. Table 1 presents the torrefaction performance results from the macro-TGA system operated with increased sample mass per crucible, i.e. from ~1 g to ~5 g. Across the range of initial sample mass from ~19 g to ~95 g, the mass yield varied < 1% (absolute), energy densification index varied from 1.25 to 1.28 (~2.5% relative), and no significant impacts were observed on heating value, volatile matter, ash and fixed carbon results. Thus, the macro-TGA may be used to perform torrefaction tests with similar sample processing capacity as the fixed bed reactor. The varied sample mass torrefaction tests were repeated with uncovered crucibles to investigate the impact on torrefaction performance. The results (Table S4) indicate that without a crucible cover, the varied sample loading mass (1–5 g) results in variation in torrefied product properties of 10–20% (relative).

Fig. 10 shows the sample mass change during the pod torrefaction process from 184 to 281 °C with 20 °C/min heating rate, 60 min residence time, and 60 min cooling period in covered crucibles; the plot includes mass loss data for all 19 crucibles. The physicochemical properties and chemical structure of these torrefied materials were also analyzed and reported in Tables S5 and S6, and Figure S1. As with the fixed bed reactor, the mass yield of the torrefaction process approaches targeted values, 70%, when the torrefaction temperature is approximately 230 °C. The mass yield at higher temperature, i.e. 240, 254, and 281 °C, reaches 70% when the residence time is approximately 40, 15, and 5 min, respectively, if the mass loss during the cooling process is not considered. As biomass torrefaction strongly depends on the chemical decomposition of hemicellulose, the torrefaction temperature has a greater impact on the torrefied product than residence time, moisture

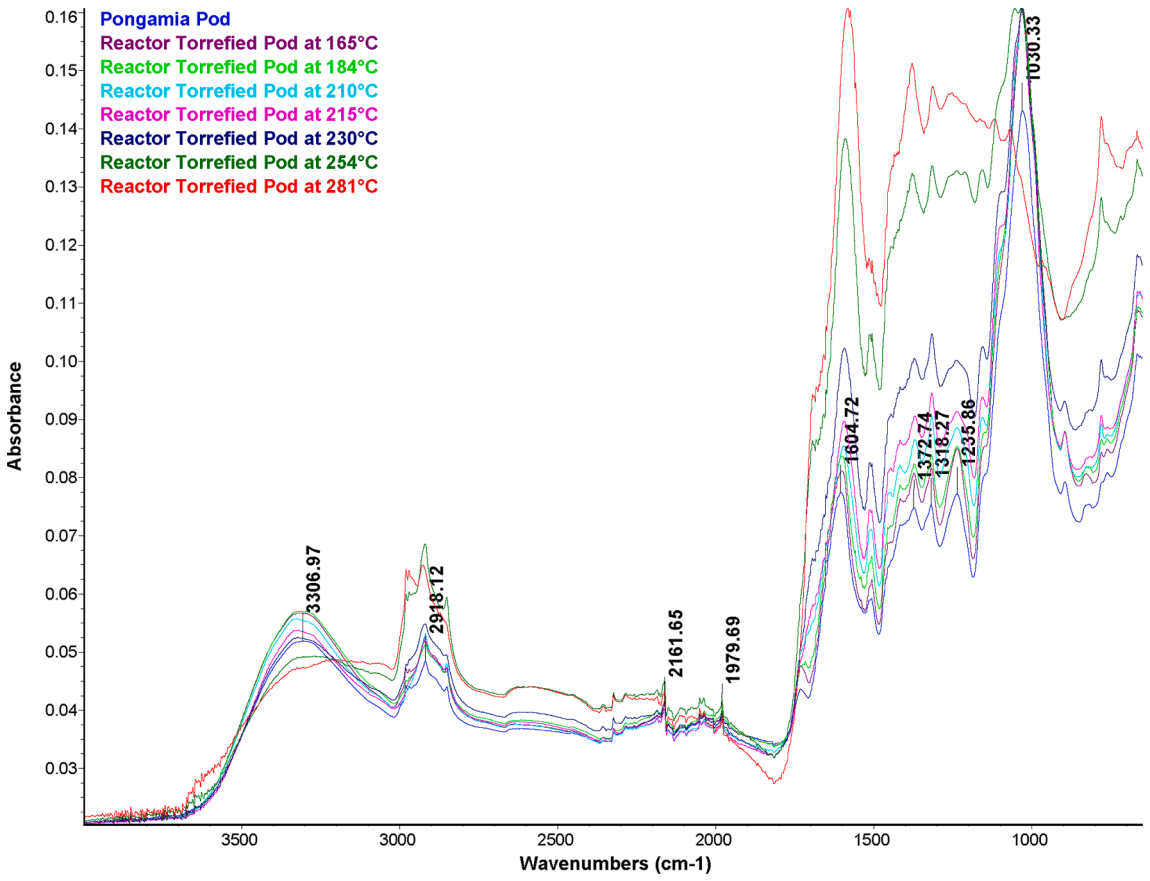

Fig. 9. FT-IR spectra of raw and torrefied pods.

Table 1
Comparison of torrefied pongamia pods' (≤2 mm) properties produced with a LECO TGA-801, covered crucibles, and different starting sample masses. TGA-801 operating conditions ramped from 25 to 225 °C at a rate of 20 °C/min, 60 min hold, under a nitrogen environment.

Mass	1.0 g	2.0 g	3.0 g	4.0 g	5.0 g
My (%)	72.74 ± 0.26	73.25 ± 0.19	73.67 ± 0.18	73.60 ± 0.19	73.68 ± 0.16
HHV (MJ/kg)	20.42 ± 0.31	20.57 ± 0.07	20.17 ± 0.39	20.89 ± 0.07	20.77 ± 0.06
Ey (%)	91.02 ± 1.39	92.33 ± 0.32	91.04 ± 1.75	94.19 ± 0.31	93.79 ± 0.26
Ied	1.25 ± 0.02	1.26 ± 0.00	1.24 ± 0.02	1.28 ± 0.00	1.27 ± 0.00
VM wt%	65.01 ± 0.11	65.4 ± 0.01	65.12 ± 0.06	65.57 ± 0.15	65.34 ± 0.19
Ash wt%	7.97 ± 0.18	8.15 ± 0.10	7.48 ± 0.92	7.8 ± 0.21	8.29 ± 0.10
FC wt%	27.02 ± 0.27	26.45 ± 0.11	27.4 ± 0.80	26.63 ± 0.07	26.37 ± 0.20

Note: (1) VM and FC are volatile matter and fixed carbon content on dry basis, respectively; (2) FC was calculated by subtracting the VM and ash percentages from 100; (3) mass yield is average result of 19 analysis, and all other results are given as the mean ± standard error of three analyses.

content, and particle size [7]. Macro-TGA was also employed to conduct preliminary tests on the torrefaction process with zero residence, which may help to reduce the overall processing time and cost. Fig. 11 displays the thermogravimetric curve of torrefaction processes performed at 280, 290, 295 and 300 °C. The mass yield reaches 70% using a torrefaction temperature of 295 °C, no hold time, and 60 min cooling. It should be noted that the cooling period is necessary for the process to remove the excessive smoke generated when residence time is zero.

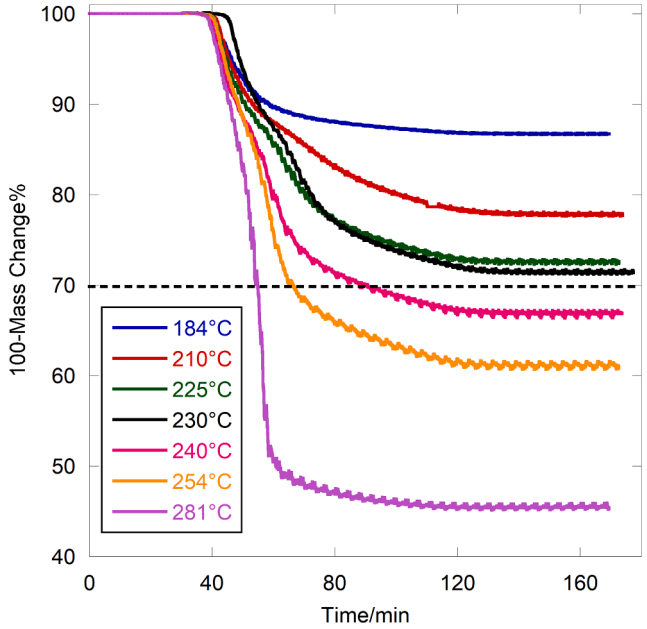

Fig. 10. Thermogravimetric curve of the macro-TGA torrefaction tests with 20 °C/min heating rate, 60 min residence time, and 60 min cooling period.

3.3. Fixed bed reactor vs. macro-TGA

In comparison with the fixed bed reactor, the commercially available macro-TGA has many advantages including: (1) simplified sample loading and unloading, (2) easier to operate, and (3) capable of semi-

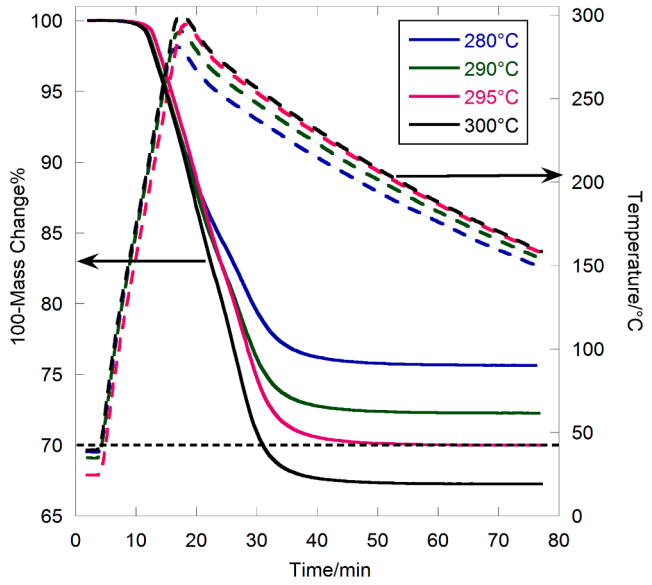

Fig. 11. Thermogravimetric curve for the macro-TGA torrefaction tests without residence time.

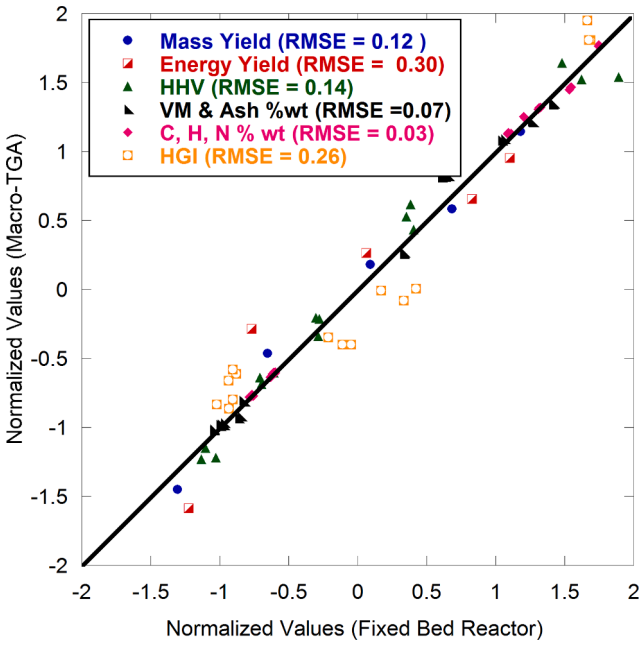

Fig. 12. Comparison of the macro-TGA and fixed bed reactor performance: normalized experimental values.

continuously monitoring of mass loss. The disadvantage is that the product gases are not swept from the covered crucibles during the torrefaction process as would be the case at larger scales. The torrefaction performance of the macro-TGA was compared with that of the fixed bed reactor (Fig. 12). The data in Fig. 12, including mass and energy yield, HHV, volatile matter and ash content based on proximate analysis, C, H, and N content, and HGI, were normalized and the overall RMSE = 0.13. This comparison suggests that the TGA 801 can be used as a rapid screening tool for biomass torrefaction.

4. Conclusion

Torrefaction of pongamia pods grown on the island of Oahu in Hawaii was performed to study the impact of the torrefaction processes on the fuel characteristic of the pods for potential use in thermochemical conversion applications. The physicochemical properties of the torrefied pods were determined and compared with that of bituminous coal. The use of a commercially available macro-TGA as a rapid screening torrefaction tool was also evaluated.

Based on the analysis, the following conclusions were drawn:

- The mass and energy yield and energy densification index of the torrefaction process for pongamia pods reach the targeted values, i.e. 70%, 90% and 1.30, respectively, using torrefaction temperatures of 220–230 °C.
- The torrefied pods possess similar fuel qualities as bituminous coal when the torrefaction temperature is 281 °C.
- A small fraction of sulfur can be released from the pod during torrefaction, but the torrefied pods are enriched in sulfur compared to the parent material; the overall sulfur content of the torrefied pods is much lower than the coal.
- The release of chlorine was not observed during torrefaction, and the elevated potassium and chlorine content of the torrefied pods will require management to avoid deposition and fouling when utilized for combustion or gasification.
- The macro-TGA was capable of similar loading capacity, ~100 g, as the fixed bed reactor, and torrefied pods generated by macro-TGA possess similar fuel properties as that from the fixed bed reactor.
- The macro-TGA is demonstrated as a fast screening tool to generate torrefaction samples under varied process parameters of temperature, heating rate, and hold time.
- Although the torrefaction process can improve fuel qualities of pongamia pod, further research to reduce their alkali metals and chlorine contents should be pursued.
- More investigations are needed on the pretreatment and thermochemical conversion of other residues derived from pongamia oil processing, such as truck of aged trees and seed cake.

CRediT authorship contribution statement

Jinxia Fu: Conceptualization, Methodology, Investigation, Supervision, Visualization, Writing - original draft. **Sabrina Summers:** Investigation, Formal analysis, Writing – review & editing. **Scott Q. Turn:** Conceptualization, Project administration, Writing – review & editing, Funding acquisition. **William Kusch:** Resources, Writing – review & editing.

Declaration of Competing Interest

The authors declare that they have no known competing financial interests or personal relationships that could have appeared to influence the work reported in this paper.

Acknowledgement

This research was funded in part by the U.S. Federal Aviation Administration Office of Environment and Energy through ASCENT, the FAA Center of Excellence for Alternative Jet Fuels and the Environment, project 001 through FAA Award Number 13-C-AJFE-UH under the supervision of James Hileman and Nathan Brown. Any opinions, findings, conclusions or recommendations expressed in this material are those of the authors and do not necessarily reflect the views of the FAA.

Funding was also provided by Hawaii's Environmental Response, Energy, and Food Security Tax (HRS Sec. 243-3.5 "Barrel Tax") through the Hawaii Natural Energy Institute's Energy Systems Development Special Fund, Grant N-00014-16-1-2116 from the Office of Naval Research, and project number 11910-IWVU from the Undergraduate Research Opportunities Program at the University of Hawaii at Mānoa.

The authors thank (1) Dr. Kristin C. Lewis (U.S. Dept. of Transportation, Volpe Center) for her thorough review of the manuscript prior

to submission and her suggestions for improvement; (2) Dr. Xiao Zhang's research group (Washington State University) for conducting summative analysis of pongamia pods.

Appendix A. Supplementary data

Supplementary data to this article can be found online at https://doi.org/10.1016/j.fuel.2021.120260.

References

[1] IEA. World Energy Outlook 2019: https://www.iea.org/reports/world-energy-outlook-2019; 2019. [Accessed April 20 2020].
[2] Sharma HB, Sarmah AK, Dubey B. Hydrothermal carbonization of renewable waste biomass for solid biofuel production: A discussion on process mechanism, the influence of process parameters, environmental performance and fuel properties of hydrochar. Renew Sustain Energy Rev 2020;123:109761.
[3] Wang T, Zhai Y, Zhu Y, Li C, Zeng G. A review of the hydrothermal carbonization of biomass waste for hydrochar formation: Process conditions, fundamentals, and physicochemical properties. Renew Sustain Energy Rev 2018;90:223–47.
[4] van der Stelt MJC, Gerhauser H, Kiel JHA, Ptasinski KJ. Biomass upgrading by torrefaction for the production of biofuels: A review. Biomass Bioenergy 2011;35(9):3748–62.
[5] Bergman PCA. Torrefaction for biomass co-firing in existing coal-fired power stations BIOCOAL. In: Energieonderzoek Centrum N, ed.; 2005.
[6] Chen W-H, Peng J, Bi XT. A state-of-the-art review of biomass torrefaction, densification and applications. Renew Sustain Energy Rev 2015;44:847–66.
[7] Niu Y, Lv Y, Lei Y, Liu S, Liang Y, Wang D, et al. Biomass torrefaction: properties, applications, challenges, and economy. Renew Sustain Energy Rev 2019;115:109395.
[8] Chen W-H, Kuo P-C. Torrefaction and co-torrefaction characterization of hemicellulose, cellulose and lignin as well as torrefaction of some basic constituents in biomass. Energy 2011;36(2):803–11.
[9] Chen W-H, Kuo P-C. A study on torrefaction of various biomass materials and its impact on lignocellulosic structure simulated by a thermogravimetry. Energy 2010;35(6):2580–6.
[10] Prins MJ, Ptasinski KJ, Janssen FJJG. Torrefaction of wood: Part 1. Weight loss kinetics. J Anal Appl Pyrol 2006;77(1):28–34.
[11] Yang Y, Sun M, Zhang M, Zhang K, Wang D, Lei C. A fundamental research on synchronized torrefaction and pelleting of biomass. Renewable Energy 2019;142:668–76.
[12] Manouchehrinejad M, Mani S. Torrefaction after pelletization (TAP): Analysis of torrefied pellet quality and co-products. Biomass Bioenergy 2018;118:93–104.
[13] Chang S, Zhao Z, Zheng A, He F, Huang Z, Li H. Characterization of Products from Torrefaction of Sprucewood and Bagasse in an Auger Reactor. Energy Fuels 2012;26(11):7009–17.
[14] Toscano G, Pizzi A, Foppa Pedretti E, Rossini G, Ciceri G, Martignon G, et al. Torrefaction of tomato industry residues. Fuel 2015;143:89–97.
[15] Prins MJ, Ptasinski KJ, Janssen FJJG. Torrefaction of wood: Part 2. Analysis of products. J Anal Appl Pyrol 2006;77(1):35–40.
[16] Bridgeman TG, Jones JM, Williams A, Waldron DJ. An investigation of the grindability of two torrefied energy crops. Fuel 2010;89(12):3911–8.
[17] Couhert C, Salvador S, Commandré JM. Impact of torrefaction on syngas production from wood. Fuel 2009;88(11):2286–90.
[18] Andersen LK, Morgan TJ, Boulamanti AK, Álvarez P, Vassilev SV, Baxter D. Quantitative X-ray Fluorescence Analysis of Biomass: Objective Evaluation of a Typical Commercial Multi-Element Method on a WD-XRF Spectrometer. Energy Fuels 2013;27(12):7439–54.
[19] Wen R, Lv HN, Jiang Y, Tu PF. Anti-inflammatory Flavanones and Flavanols from the Roots of Pongamia pinnata. Planta Med 2018;84(16):1174–82.
[20] Chakraborty SK, Chandel NS, Kotwaliwale N, Sadvatha RH, Fasake VD, Mishra SS, et al. Characterisation of Properties for Karanj (Pongamia pinnata) Seeds and Kernels in Relation to Bulk Handling and Processing Applications. Agric Res 2018;7(3):280–9.
[21] Chopade VV, et al. *Pongamia pinnata*: Phytochemical constituents, Traditional uses and Pharmacological properties: A review. Int J Green Pharm 2008;2(2):72–5.
[22] Sagar R, Dumka VK, Singh H, Singla S. Evaluation of antipyretic, muscle relaxant and neurobehavioural activities of various leaf extracts of Pongamia pinnata L. Ann Phytomedicine 2018;7(2):98–101.
[23] Bhuvaneswari TK, Vasantha VS, Jeyaprabha C. Pongamia Pinnata as a Green Corrosion Inhibitor for Mild Steel in 1N Sulfuric Acid Medium. Silicon 2018;10(5):1793–807.
[24] Dwivedi G, Sharma MP. Prospects of biodiesel from Pongamia in India. Renew Sustain Energy Rev 2014;32:114–22.
[25] Singh SP, Singh D. Biodiesel production through the use of different sources and characterization of oils and their esters as the substitute of diesel: A review. Renew Sustain Energy Rev 2010;14(1):200–16.
[26] Aina Akmal Mohd N, Siti Nurul Najiha O, Pei Teng L, Shankar M, Mohd Farooq S, Mahendran S. Molecules of Interest – Karanjin – A Review. Pharmacogn J 2020;12(4).
[27] Doshi P, Srivastava G, Pathak G, Dikshit M. Physicochemical and thermal characterization of nonedible oilseed residual waste as sustainable solid biofuel. Waste Manage 2014;34(10):1836–46.
[28] Soren NM, Sharma AK, Sastry VRB. Biochemical and histopathological changes in sheep fed different detoxified karanj (Pongamia glabra) seed cake as partial protein supplements. Anim Nutr 2017;3(2):164–70.
[29] Singh P, Garg AK, Agrawal DK, Ravi U. Performance of lambs fed expeller pressed and solvent extracted karanj (Pongamia pinnata) oil cake. Anim Feed Sci Technol 2000;88(1–2):121–8.
[30] Masawat N, Atong D, Sricharoenchaikul V. Thermo-kinetics and product analysis of the catalytic pyrolysis of Pongamia residual cake. J Environ Manage 2019;242:238–45.
[31] Dhanavath KN, Shah K, Islam MS, Ronte A, Parthasarathy R, Bhargava SK, et al. Experimental investigations on entrained flow gasification of Torrefied Karanja Press Seed Cake. J Environ Chem Eng 2018;6(1):1242–9.
[32] Usharani KV, Dhananjay N, Manjunatha RL. *Pongamia pinnata* (L.): Composition and advantages in agriculture: A review. J Pharmacogn Phytochem 2019;8(3):2181–7.
[33] Naik DK, Ahmed MS, Aniya V, Parthasarathy R, Satyavathi B. Torrefaction assessment and kinetics of deoiled karanja seed cake. Environ Prog Sustain Energy 2017;36(3):758–65.
[34] Naik D, et al. Pre-treatment of karanja biomass via torrefaction: Effect on syngas yield and char composition. Asia Pacific Confederation of Chemical Engineering Congress 2015 2015; Melbourne: Engineers Australia:1174-85.
[35] Ujjinappa S, Sreepathi LK. Production and quality testing of fuel briquettes made from pongamia and tamarind shell. Sadhana-Acad Proc Eng Sci 2018;43(4):7.
[36] Patil SA, Patil SK, Sartape AS, Bhise SC, Vadiyar MM, Anuse MA, et al. A Pongamia pinnata pods based activated carbon as an efficient scavenger for adsorption of toxic Co(II): kinetic and thermodynamic study. Separation Science and Technology:15.
[37] ASTM D409/D409M - 16: Standard Test Method for Grindability of Coal by the Hardgrove-Machine Method. ASTM Internationa. West Conshohocken, PA, 2016.
[38] Li D. Impact of torrefaction on grindability, hydrophobicity and fuel characteristics of biomass relevant to Hawai'i. [Honolulu] : [University of Hawaii at Manoa], [December 2015]; 2015.
[39] Asadullah M, Adi AM, Suhada N, Malek NH, Saringat MI, Azdarpour A. Optimization of palm kernel shell torrefaction to produce energy densified bio-coal. Energy Convers Manage 2014;88:1086–93.
[40] Nyakuma BB, Ahmad A, Johari A, Abdullah TAT, Oladokun O, Al-Shatri AH, et al. Preliminary torrefaction of oil palm empty fruit bunch pellets. E3S web of conferences 2019;90:1014.
[41] ASTM E1756 - 08: Standard Test Method for Determination of Total Solids in Biomass. ASTM Internationa. West Conshohocken, PA, 2015.
[42] ASTM E1755 - 01: Standard Test Method for Ash in Biomass. ASTM Internationa. West Conshohocken, PA, 2015.
[43] ASTM E872 - 82: Standard Test Method for Volatile Matter in the Analysis of Particulate Wood Fuels. ASTM Internationa. West Conshohocken, PA, 2019.
[44] ASTM D4809-18: A. Standard Test Method for Heat of Combustion of Liquid Hydrocarbon Fuels by Bomb Calorimeter (Precision Method). ASTM Internationa. West Conshohocken, PA, 2018.
[45] Sluiter A, Hames B, Ruiz R, Scarlata C, Sluiter J, Templeton D, et al. Determination of structural carbohydrates and lignin in biomass laboratory analytical procedure (LAP): issue date, 4/25/2008. Golden, Colo: National Renewable Energy Laboratory; 2012.
[46] Morgan TJ, George A, Boulamanti AK, Álvarez P, Adanouj I, Dean C, et al. Quantitative X-ray Fluorescence Analysis of Biomass (Switchgrass, Corn Stover, Eucalyptus, Beech, and Pine Wood) with a Typical Commercial Multi-Element Method on a WD-XRF Spectrometer. Energy Fuels 2015;29(3):1669–85.
[47] Morgan TJ, Andersen LK, Turn SQ, Cui H, Li D. XRF Analysis of Water Pretreated/Leached Banagrass to Determine the Effect of Temperature, Time, and Particle Size on the Removal of Inorganic Elements. Energy Fuels 2017;31(8):8245–55.
[48] Chen H, Chen X, Qiao Z, Liu H. Release and transformation characteristics of K and Cl during straw torrefaction and mild pyrolysis. Fuel 2016;167:31–9.
[49] Saleh SB, Flensborg JP, Shoulaifar TK, Sárossy Z, Hansen BB, Egsgaard H, et al. Release of Chlorine and Sulfur during Biomass Torrefaction and Pyrolysis. Energy Fuels 2014;28(6):3738–46.
[50] Knudsen JN, Jensen PA, Lin W, Frandsen FJ, Dam-Johansen K. Sulfur Transformations during Thermal Conversion of Herbaceous Biomass. Energy Fuels 2004;18(3):810–9.
[51] Guo B, Ghalambor A. Chapter 8 - Dehydration. In: Guo B, Ghalambor A, editors. Natural Gas Engineering Handbook (Second Edition). Gulf Publishing Company; 2005. p. 143–71.
[52] Yang H, Yan R, Chen H, Lee DH, Zheng C. Characteristics of hemicellulose, cellulose and lignin pyrolysis. Fuel 2007;86(12):1781–8.
[53] Xin S, Mi T, Liu X, Huang F. Effect of torrefaction on the pyrolysis characteristics of high moisture herbaceous residues. Energy 2018;152:586–93.
[54] Turn SQ, Kinoshita CM, Ishimura DM, Zhou J. The fate of inorganic constituents of biomass in fluidized bed gasification. Fuel 1998;77(3):135–46.
[55] Turn SQ, Kinoshita CM, Ishimura DM. Removal of inorganic constituents of biomass feedstocks by mechanical dewatering and leaching. Biomass Bioenergy 1997;12(4):241–52.